Kinetic Stabilization and Fusion of Apolipoprotein A-2:DMPC Disks: Comparison with apoA-1 and apoC-1

Shobini Jayaraman, Donald L. Gantz, and Olga Gursky
Department of Physiology and Biophysics, Boston University School of Medicine, Boston, Massachusetts

ABSTRACT Denaturation studies of high-density lipoproteins (HDL) containing human apolipoprotein A-2 (apoA-2) and dimyristoyl phosphatidylcholine indicate kinetic stabilization. Circular dichroism (CD) and light-scattering melting curves show hysteresis and scan rate dependence, indicating thermodynamically irreversible transition with high activation energy E_a. CD and light-scattering data suggest that protein unfolding triggers HDL fusion. Electron microscopy, gel electrophoresis, and differential scanning calorimetry show that such fusion involves lipid vesicle formation and dissociation of monomolecular lipid-poor protein. Arrhenius analysis reveals two kinetic phases, a slower phase with $E_{a,slow} = 60$ kcal/mol and a faster phase with $E_{a,fast} = 22$ kcal/mol. Only the fast phase is observed upon repetitive heating, suggesting that lipid-poor protein and protein-containing vesicles have lower kinetic stability than the disks. Comparison of the unfolding rates and the melting data recorded by differential scanning calorimetry, CD, and light scattering indicates the rank order for the kinetic disk stability, apoA-1 $>$ apoA-2 $>$ apoC-1, that correlates with protein size rather than hydrophobicity. This contrasts with the tighter association of apoA-2 than apoA-1 with mature HDL, suggesting different molecular determinants for stabilization of model discoidal and plasma spherical HDL. Different effects of apoA-2 and apoA-1 on HDL fusion and stability may reflect different metabolic properties of apoA-2 and/or apoA-1-containing HDL.

INTRODUCTION

High-density lipoproteins (HDLs) are heterogeneous complexes of lipids and specific proteins (termed *exchangeable apolipoproteins*) that mediate cholesterol removal from peripheral tissues to the liver via the process termed *reverse cholesterol transport* (Fielding and Fielding, 1995). This function accounts, in part, for the anti-atherogenic action of HDL and its major protein, apolipoprotein A-1 (apoA-1, 243 aa) (Barter and Rye, 1996). Plasma levels of HDL and apoA-1 correlate inversely with the incidence of coronary artery disease, yet the role of the second major HDL protein, apoA-2, is less clear (Hedrick and Lusis, 1994; Blanco-Vaca et al., 2001; Tailleux et al., 2002). ApoA-1 and apoA-2 comprise ~70% and 20% of the total HDL protein content, respectively. ApoA-2 (a 77-residue polypeptide that forms an S-S linked dimer of 17.4 kDa in humans) reduces the anti-atherogenic effects of HDL and modulates HDL metabolism via diverse mechanisms. These include activation or inhibition of plasma enzymes that are essential in reverse cholesterol transport (Forte et al., 1995; Labeur et al., 1998; Blanco-Vaca et al., 2001; Hedrick et al., 2001; Boucher et al., 2004), and direct or indirect effects of apoA-2 on HDL cell receptors (Blanco-Vaca et al., 2001; De Beer et al., 2001; Rinninger et al., 2003), transporters (Remaley et al., 2001), and apoA-1 (Hedrick et al., 2001; Rye et al., 2003). ApoA-2 inhibits enzymatic HDL remodeling, such as HDL fusion and apoA-1 dissociation (Calabresi et al., 1996; Pussinen et al., 1997; Rye et al., 2003), and reduces the rate of apoA-1 transfer among HDL (Cheung et al., 1992; Rye and Barter, 2004). Furthermore, apoA-2 can displace apoA-1 from HDL (Durbin and Jonas, 1997; Labeur et al., 1998) and is released from mature plasma HDL at higher temperatures or higher denaturant concentrations than apoA-1 (Nichols et al., 1976; Tall et al., 1977). Therefore, apoA-2 is believed to be more strongly associated with plasma HDL than apoA-1 (Forte et al., 1995; Durbin and Jonas, 1997).

ApoA-1, apoA-2, and other exchangeable apolipoproteins have evolved from a common ancestor that is related to the smallest human apolipoprotein, apoC-1 (57 aa) (Luo et al., 1986). The amino acid sequences of these proteins are comprised of tandem 11/22-residue repeats that have high propensity to form amphipathic α-helices with distinct charge distribution and large apolar faces that bind lipid (Segrest et al., 1992). ApoA-2 has particularly large apolar helical faces (50% of the surface as compared to ~30% in apoA-1 and apoC-1) which, along with higher hydrophobicity of these faces, is thought to account for stronger association of apoA-2 with HDL (Brasseur et al., 1992; Forte et al., 1995). In their lipid-free state, apoA-2 and other exchangeable apolipoproteins form marginally stable molten globule with substantial helix content but nonspecific tertiary structures (Gursky and Atkinson, 1996a,b). X-ray crystal structure of lipid-free apoA-2 comprises a bundle of nearly parallel helices that opens upon lipid binding (Kumar et al., 2002). Lipid binding stabilizes apoA-2 and other apolipoproteins against denaturation and proteolysis via the

Submitted November 9, 2004, and accepted for publication January 21, 2005.

Address reprint requests to Dr. Olga Gursky, Dept. of Physiology and Biophysics, Boston University School of Medicine, W329, 715 Albany St., Boston, MA 02118. Tel.: 617-638-7894; Fax: 617-638-4041; E-mail: gursky@bu.edu.

Abbreviations used: LpA-1, HDL containing apoA-1 but not apoA-2; LpA-2, HDL containing apoA-2 but not apoA-1; LpA-1/A-2, HDL containing both apoA-1 and apoA-2.

0006-3495/05/04/2907/12 $2.00

doi: 10.1529/biophysj.104.055921

mechanism addressed in this and in our earlier studies (Gursky et al., 2002; Mehta et al., 2003a,b; Fang et al., 2003; Jayaraman et al., 2004).

Nascent HDL form discoidal particles comprised of cholesterol-containing phospholipid bilayer and the amphipathic protein helices that are wrapped around the disk circumference in a beltlike conformation (Lund-Katz et al., 2003, and references therein) and confer disk stability and solubility. After cholesterol esterification by lecithin:cholesterol acyltransferase (LCAT), disks are converted into spherical HDL containing an apolar core of cholesterol esters and triglycerides and an amphipathic surface of proteins and phospholipids. These mature HDL, which are further remodeled by plasma enzymes, form distinct subclasses differing in size, composition and metabolic properties (reviewed by Rye and Barter, 2004). The majority of HDL contains both apoA-1 and apoA-2 (LpA-1/A-2); most of the remaining particles contain apoA-1 but not apoA-2 (LpA-1), and a small fraction contains only apoA-2 (LpA-2) (Cheung and Albers, 1984; Pastier et al., 2001). The formation of LpA-1/A-2 has been proposed to involve LCAT-induced fusion of the precursor particles containing apoA-1 and apoA-2 (Clay et al., 2000). Here, we use reconstituted discoidal HDL as a model for the analysis of fusion and stability of nascent HDL.

Our studies of model discoidal (Gursky et al., 2002; Mehta et al., 2003a; Fang et al., 2003) and plasma spherical HDL (Mehta et al., 2003b; Jayaraman et al., 2004), supported by the earlier studies of apoA-1:DMPC disks (Reijngoud and Phillips, 1982; Epand, 1982; Surewicz et al., 1986), have revealed a kinetic mechanism of HDL stabilization. By using model disks comprised of apoC-1 and DMPC, we showed that the heat-induced protein unfolding is a slow thermodynamically irreversible (or non-equilibrium) transition. By definition, such a transition has non-equal probability to proceed in forward and reverse directions, and thus is pathway-dependent; it does not necessarily involve irreversible chemical changes. The thermodynamically irreversible step in disk denaturation is protein unfolding/dissociation and disk fusion that compensates for the reduction in the particle surface, leading to a high kinetic barrier for the disk denaturation (Gursky et al., 2002). Mature human plasma HDL and LDL are also stabilized by kinetic barriers, suggesting that such barriers provide a universal natural strategy for lipoprotein stabilization (Mehta et al., 2003b; Jayaraman et al., 2004, 2005). We proposed that the kinetic barriers are functionally important, since they maintain structural integrity of lipoproteins, inhibit spontaneous interconversions among lipoprotein subclasses, and thereby modulate lipoprotein metabolism and lifetime in plasma.

In this work, we analyze kinetic stability of apoA-2:DMPC disks and compare it with the stability of similar disks containing apoA-1 or apoC-1; since these lipoproteins are stabilized by kinetic factors, their relative thermodynamic stability has not been determined. The results help to elucidate the role of apolipoprotein size and hydrophobicity for HDL stability, to uncouple apolipoprotein unfolding, dissociation, and lipoprotein fusion, and thereby gain a better insight into molecular determinants for the structural stability and fusion of HDL disks and spheres.

MATERIALS AND METHODS

Lipoprotein preparation and characterization

Single-donor HDLs were isolated from EDTA-treated human plasma by density gradient centrifugation in the range 1.08–1.21 g/ml (Schumaker and Puppione, 1986). After HDL de-lipidation by guanidinium hydrochloride (Gdm HCl), apoA-1, and apoA-2 were isolated by FPLC as described in Wetterau and Jonas (1982). The protein purity assessed by SDS gel electrophoresis was 95%. Purified proteins were dissolved in 8 M Urea and refolded by dialysis as described in Gursky and Atkinson (1996). The standard buffer was 10 mM Na phosphate, 0.02% NaN_3, pH 7.8. The stock solution of 0.1–0.5 mg/ml protein concentration was stored in the dark at 4°C and was used in four weeks, during which no protein degradation was detected. Apolipoproteins obtained by this method retain full biological activity (Wetterau and Jonas, 1982).

Complexes of dimyristoyl phosphatidylcholine (DMPC; 95+% purity) with apoA-1 or apoA-2 were obtained by spontaneous reconstitution using protein/lipid ratio 1:4 mg/mg and overnight incubation at 24°C, followed by centrifugation at 13,000 rpm for 1.5 h to remove excess lipid. Disk formation was confirmed by negative staining electron microscopy (EM) and non-denaturing gel electrophoresis which showed no free protein. In addition, apoA-2:DMPC disks were prepared by cholate dialysis (Jonas, 1986); EM, gel electrophoresis, and spectroscopic data of these disks and of the disks formed by spontaneous reconstitution were similar.

Non-denaturing gel electrophoresis of lipid-free and DMPC-associated proteins was carried out by using 8–25% polyacrylamide gradient gel (PHAST system, Pharmacia, Peapack, NJ) with Coomassie staining. Despite limited accuracy in the particle size determination and limited resolution, this system facilitates observation of lipoproteins, lipid-free and lipid-poor proteins on the same gel and is widely used for lipoprotein analysis (Davidson et al., 1995; Sparks et al., 1999). Particle diameters were assessed from comparison with protein markers with known Stokes radii and were confirmed by EM measurements.

Protein-lipid complexes were visualized by negative staining EM in a CM12 transmission electron microscope (Philips Electron Optics, Eindhoven, the Netherlands) as described (Gursky et al., 2002). The average disk diameters were determined from EM images with an accuracy of 0.2 nm using 200–400 particles.

Circular dichroism spectroscopy and light scattering

Circular dichroism (CD) and light-scattering data were recorded using AVIV-215 spectrometer (AVIV Biomedical, Lakewood, NJ) with fluorescence accessory and Pelletier temperature control. Far-UV CD spectra (185–250 nm) were recorded from solutions of 20 μg/ml protein concentration placed in 5-mm-pathlength cells, which are standard condition in our CD experiments. In addition, CD spectra of DMPC-bound apoA-2 were recorded from solutions of 5–600 μg/ml protein concentration placed in 10–0.5-mm cells. The spectra were recorded with 1 nm step, 15–60 s accumulation time. After the buffer baseline subtraction, the data were normalized to protein concentration and expressed as molar residue ellipticity, $[\Theta]$. No changes in $[\Theta]$ were detected with changes in the protein concentration in the range explored (5–600 μg/ml). The α-helix content was estimated from the value of $[\Theta]$ at 222 nm (Mao and Wallace, 1984). ORIGIN software was used for the data analysis and display (OriginLab, Northampton, MA).

The melting data, $\Theta_{222}(T)$, were recorded at 222 nm during sample heating and cooling from 5–98°C at various scan rates from 1.34–0.193 K/min (80–11 K/h) as described in Gursky et al. (2002). Fluorescence accessory was used to record 90° light scattering simultaneously with the CD. This allowed monitoring relative changes in the light scattering due to heat-induced changes in the particle size and morphology.

The kinetic CD data, $\Theta_{222}(t)$, were recorded at 222 nm in temperature-jump (T-jump) experiments from 25°C to 70–95°C as described in Gursky et al. (2002), using 20–30 s accumulation time per data point. The data were approximated by a multiexponential:

$$\Theta_{222}(t) = A_0 + A_1 \exp(-t/\tau_1) + A_2 \exp(-t/\tau_2) + \ldots.$$

Here τ_1, τ_2 are the exponential relaxation times, A_1, A_2 are the amplitudes, and A_0 is the value of Θ_{222} at $t \rightarrow \infty$. Thermal denaturation of apoA-2:DMPC disks showed biphasic kinetics. Arrhenius plots $\ln(\tau)$ versus $1/T$ for the two kinetic phases where obtained from the relaxation times $\tau(T)$ measured at 70–95°C. The activation energy E_a was determined from the slope of these plots with the accuracy of 5–8 kcal/mol, which includes the fitting errors and the deviations among different data sets.

The kinetic CD data were also recorded in denaturant-jump experiments with the disks. Protein unfolding was triggered by an increase in guanidinium hydrochloride (Gdm HCl) concentration from 0 M to 1–6 M. The resulting $\Theta_{222}(t)$ data, which showed CD changes during the dead-time of the experiment (<1 min), did not yield a reliable exponential fit and thus were not used for quantitative analysis.

Differential scanning calorimetry

An upgraded MC-2 microcalorimeter (Microcal, Amherst, MA) was used to record excess heat capacity of the apoA-2:DMPC complexes. The $C_p(T)$ data were recorded from degassed protein and/or buffer solutions upon repetitive heating from 5 to 100°C at a rate 90 K/h, followed by cooling and incubation at 24°C. Irreversibility of the high-temperature differential scanning calorimetry (DSC) transition precluded its thermodynamic analysis. After the buffer baseline subtraction, the data were normalized to protein concentration. ORIGIN software was used for the data collection, analysis, and display. All experiments in this study were repeated 3–6 times.

RESULTS

Thermal transitions in lipid-free and in DMPC-bound apoA-2

Far-UV CD data of lipid-free apoA-2 were recorded from 5 to 20 μg/ml protein solution in 10 mM Na phosphate, pH 7.6; under these conditions, the protein self-association is minimal and the predominant apoA-2 form is a disulfide-linked dimer (Swaney and O'Brien, 1978; Donovan et al., 1987). The spectrum of lipid-free apoA-2 at 25°C is invariant in the protein concentration range from 5 to 20 μg/ml and suggests 30% α-helix (Fig. 1 *A*, *open squares*). The CD melting curves at 222 nm, $\Theta_{222}(T)$, recorded during sample heating and cooling from 1 to 80°C, show that the helical structure reaches maximum at 25°C and completely unfolds upon heating as well as cooling from 25°C (Fig. 1 *B*, *open squares*). Similar unfolding below 25°C was detected in the earlier studies of human lipid-free apoA-2 at much higher protein concentration (>0.1 mg/ml), when apoA-2 is largely self-associated (Osborne et al., 1976; Ritter and Scanu, 1979; Massey et al., 1981). We attributed this unfolding to cold denaturation of the S-S linked dimer (Gursky and Atkinson, 1996b), yet other studies suggested the importance of the oligomer dissociation (Osborne et al., 1976). The observation of 30% helical structure in 5–20 μg/ml apoA-2 in the

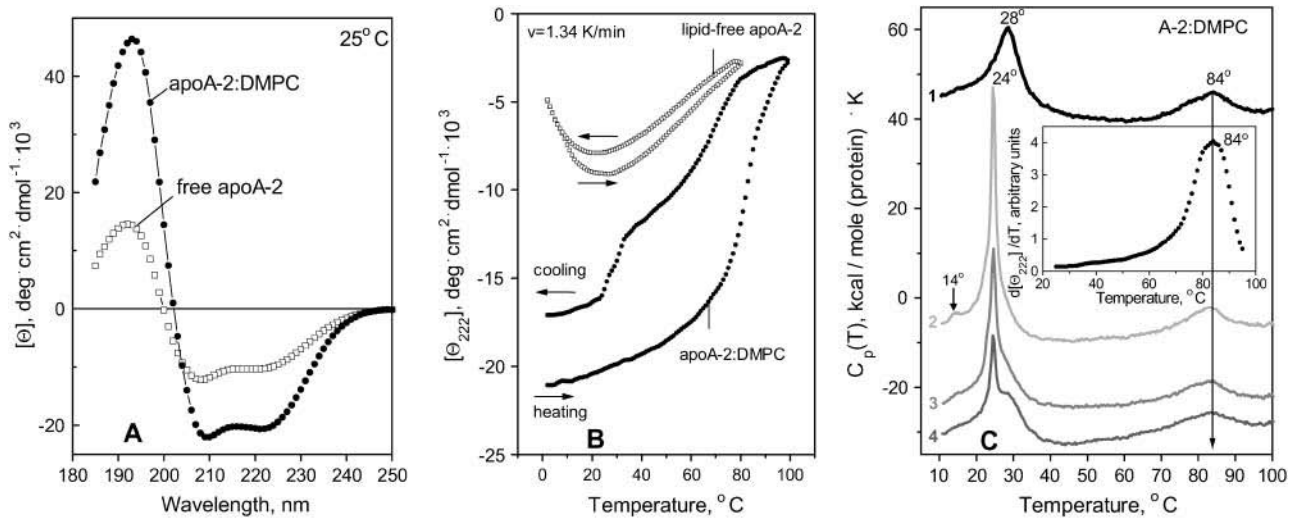

FIGURE 1 Secondary structure and thermal unfolding of apoA-2. (*A*) Far-UV CD spectra at 25°C. (*B*) Melting curves at 222 nm recorded upon heating and cooling from 5 to 98°C at a rate of 1.34 K/min (80 K/h). The data were recorded from solutions containing 20 μg/ml apoA-2 in lipid-free state (□) and on DMPC disks (●); the normalized CD data are invariant in the protein concentration range explored (5–600 μg/ml). (*C*) Excess heat capacity of apoA-2:DMPC complexes. The data were recorded from the same sample during heating from 5 to 100°C at a rate 90 K/h in four consecutive DSC scans (numbered *1–4*). After the first scan of intact disks was completed, the sample was cooled to 5°C and the instrument was equilibrated for 1 h before recording the second scan. Next, the sample was incubated at 24°C for 12 h and the third scan was recorded; finally, the sample was incubated at 24°C for 48 h and the fourth scan was recorded. The data are shifted along the *y* axis to avoid overlap; the peak temperatures are indicated. Arrow shows the midpoint of the high-temperature DSC peak. (*Inset*) First derivative $d\Theta_{222}/dT$ of the CD melting curve recorded of the disks at 80 K/h (*B*, ●).

absence of significant self-association, and the unfolding of this structure upon cooling (Fig. 1, *A* and *B*), confirm that cold denaturation is an intrinsic property of the marginally stable S-S linked apoA-2 dimer.

The CD spectrum of apoA-2:DMPC disks (Fig. 1 *A*, *solid circles*) indicates that, consistent with the earlier reports (Ritter and Scanu, 1979; Massey et al., 1981), lipid binding increases the helix content in apoA-2 to ~64%. The melting data recorded at a scan rate 1.33 K/min of lipid-free and lipid-bound protein show several important differences (Fig. 1 *B*). First, in contrast to lipid-free apoA-2, apoA-2 on DMPC disks shows no cold denaturation. Second, the heat-unfolding curve of the apoA-2:DMPC disks is sigmoidal and is shifted to higher temperatures as compared to that of free protein; thus the unfolding of free apoA-2 is complete at 80°C, well below the apparent melting temperature T_m = 84°C of the apoA-2:DMPC complexes observed at this scan rate (Fig. 1 *C*, *inset*). Third, in contrast to the reversible unfolding of lipid-free protein (indicated by the agreement between the heating and cooling CD curves in Fig. 1 *B* and by their independence of the scan rate), the heating and cooling curves of the apoA-2:DMPC complexes show hysteresis that was also observed in DMPC complexes with apoC-1 (Gursky et al., 2002; Mehta et al., 2003a) and apoA-1 (Fang et al., 2003), and is a hallmark of a non-equilibrium transition. Furthermore, the cooling curve of the apoA-2:DMPC sample shows partial protein refolding below 80°C, followed by additional refolding between 32 and 24°C, i.e., near the temperature T_c = 24°C of the liquid crystal-to-gel transition in DMPC at which apolipoprotein-lipid association is fastest (Epand, 1982). This refolding may reflect partial reconstitution of the apoA-2:DMPC complexes.

Repetitive heating and cooling of the same apoA-2:DMPC sample at 1.33 K/min (80 K/h) yields similar CD melting curves (not shown), with the apparent T_m = 84°C identical to that of intact disks. In contrast, repetitive DSC scans recorded from the same sample are significantly different. In one series of DSC experiments, the heat capacity $C_p(T)$ was recorded from the same sample during repetitive heating from 5 to 100°C followed by incubation at 24°C for 0–48 h (Fig. 1 *C*). To facilitate direct comparison of the CD and DSC data in Fig. 1, *B* and *C*, we used similar heating rates (80–90 K/h) in these experiments. The $C_p(T)$ data of intact disks shows two peaks (Fig. 1 *C*, *curve 1*). The first peak is centered at 28°C and reflects DMPC phase transition in intact disks that is not detected by CD (Fig. 1 *B*). The +4°C shift, the reduced height, and the increased width (decreased cooperativity) of this peak as compared to the sharp transition in DMPC vesicles at 24°C (Chapman, 1975) are characteristic of lipoprotein disks that have smaller cooperative lipid domains than vesicles. The second DSC peak is centered at 84°C, which is similar to the apparent T_m determined from the peak position in the first derivative of the CD melting data, $d\Theta_{222}(T)/dT$ (Fig. 1 *C*, *inset*). Consequently, the high-temperature DSC transition involves apoA-2 unfolding. Since lipid-free apoA-2 unfolds at much lower temperatures (Fig. 1 *B*, *open squares*), the protein undergoing this transition must be lipidated.

Heating of apoA-2:DMPC disks from 5 to 70°C, i.e., before the onset of the second calorimetric transition, is fully reversible and leads to no detectable changes in the subsequent DSC scans (data not shown). In contrast, heating to 100°C, i.e., beyond completion of the second calorimetric peak, leads to large changes in the subsequent scans. For example, a sample that was used to record curve 1 in Fig. 1 *C* was rapidly cooled to 5°C and scanned again from 5 to 100°C. This scan shows a sharp lipid transition at 24°C with a pretransition at 14°C that is characteristic of DMPC vesicles (*curve 2* in Fig. 1 *C*) (Chapman, 1975). Although the exact shape of this transition varies for apoA-2 samples from different plasma pools, the sharp peak at 24°C is always observed after disk heating beyond the high-temperature DSC transition, indicating disk-to-vesicle conversion in this transition. Interestingly, the midpoint and shape of the high-temperature DSC peak do not significantly change in the first and consecutive scans (*curves 1–4* in Fig. 1 *C*), consistent with the absence of such changes in repetitive CD scans. Thus the high-temperature DSC and CD transition remains invariant in the consecutive scans, yet it leads to a thermodynamically irreversible disk-to-vesicle conversion.

To test whether the heating of apoA-2:DMPC disks to 100°C followed by incubation at 24°C (where protein-DMPC binding is fastest) leads to reconstitution of intact-size disks, the sample was incubated between the consecutive DSC scans at 24°C for up to 48 h. The $C_p(T)$ data indicate a gradual reduction in the vesicle population and a concomitant increase in the disks population during incubation (Fig. 1 *C*, *curves 3* and *4*). After 48-h incubation, the disk reconstitution appears incomplete and a sharp lipid transition of reduced amplitude is detected (Fig. 1 *C*, *curve 4*). Although the time of the disk reconstitution may vary for apoA-2 from different plasma pools, the general trend is similar and shows a relatively slow vesicle-to-disk conversion. This suggests that the protein refolding detected by CD between 32 and 24°C upon relatively rapid cooling (Fig. 1 *B*, *solid circles*) mainly reflects the formation of the protein-containing vesicles rather than intact-size disks.

To assess the high- and low-molecular-weight products of the thermal disruption and reconstitution of the apoA-2:DMPC disks, we used negative staining electron microscopy and non-denaturing gel electrophoresis (Fig. 2). EM images of intact disks show particles of uniform diameters stacked on edge (Fig. 2 *A*), which result from the negative staining. The disk thickness determined from these stacks (i.e., the thickness of the DMPC bilayer) is 5.6 nm, and the average disk diameter is $\langle d \rangle$ = 11.1 nm, in agreement with the size assessed from the native gel (Fig. 2 *E*, *lane 4*). EM images show that incubation of intact disks at high temperatures leads to disk fusion into small unilamellar

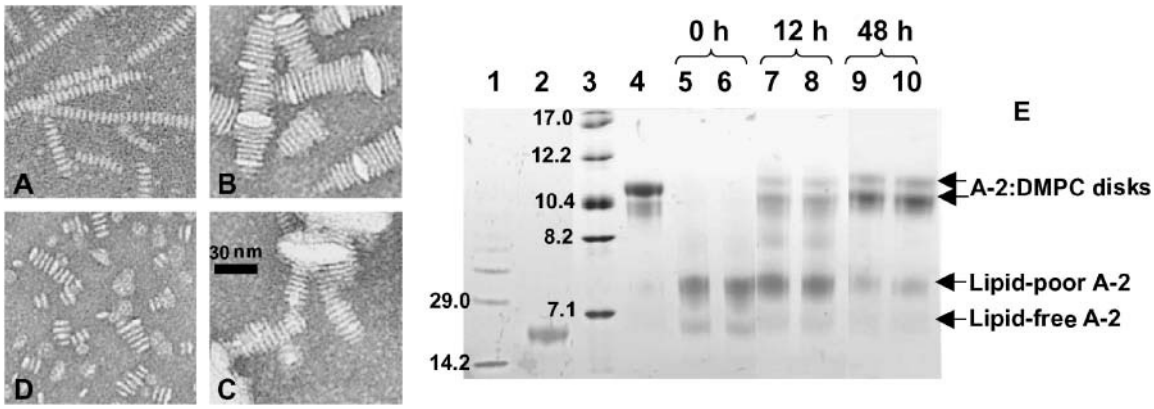

FIGURE 2 Electron micrographs and gel electrophoresis of thermally or chemically treated apoA-2:DMPC complexes. (*A*) intact disks; (*B*) disks after 30-min incubation at 75°C followed by rapid cooling to 24°C (U-shaped lipid bilayer structures characteristic of collapsed unilamellar vesicles are indicated); (*C*) disks after 30-min incubation at 95°C followed by rapid cooling to 24°C (collapsed multilamellar liposomes are indicated); and (*D*) disks after overnight incubation in 5 M Gdm HCl at 24°C. (*E*) Non-denaturing gel electrophoresis of lipid-free and DMPC-bound apoA-2. (*Lane 1*) Low molecular-weight standards (molecular weights in kDa are indicated). (*Lane 2*) Lipid-free apoA-2. (*Lane 3*) High molecular-weight standards (Stokes radii in nm are indicated). (*Lane 4*) Intact apoA-2:DMPC disks. (*Lanes 5–10*) Disks after 30-min incubation at 95°C followed by incubation at 24°C for 0 h (*5*, *6*), 12 h (*7*, *8*), and 48 h (*9*, *10*).

vesicles, followed by fusion into large, possibly multilamellar, vesicles. Thus, incubation of intact disks at 75°C for 30 min leads to disk fusion into enlarged particles that form stacks similar to disks but have larger diameters ($d \geq$ 25 nm) and occasionally form U-shaped bilayer structures typical of collapsed protein-containing vesicles (Fig. 2 *B*); incubation for longer time (2.5 h at 75°C) or at higher temperatures (30 min at 95°C) leads to an increased population of large multilamellar liposomes (Fig. 2 *C*).

Disk fusion is accompanied by dissociation of lipid-poor monomolecular apoA-2, as indicated by the low-molecular-weight band corresponding to the particle size of ~7.5 nm observed after sample exposure to high temperatures (*lanes 5* and *6* in Fig. 2 *E*). Incubation of the heat-denatured samples at 24°C leads to gradual disk reconstitution accompanied by a reduction in the amount of lipid-poor apoA-2 (Fig. 2 *E*, *lanes 7–10*). After 48-h incubation, disk reconstitution is incomplete and a significant amount of lipid-poor apoA-2 is detected (*lanes 9* and *10*). This agrees with the DSC data from an identical sample indicating that disk reconstitution after heat denaturation takes more than 48 h to complete at 24°C (Fig. 1 *C*, *curve 4*). Although the exact time of disk reconstitution varies for apA-2 from different pools, our data consistently show that the vesicle-to-disk conversion after heat denaturation of apoA-2:DMPC disks is a slow reaction that takes hours to complete at 24°C. The reaction rate is even slower above 24°C, suggesting that the heat-induced disk-to-vesicle conversion is thermodynamically irreversible.

Denaturation kinetics of apoA-2:DMPC disks

To correlate the heat-induced lipoprotein fusion with the protein unfolding and to probe the kinetics of these transitions, we recorded CD and light-scattering data at 222 nm upon sample heating and cooling at a rate from 1.33 to 0.193 K/min (Fig. 3, *A* and *B*). CD melting curves of the apoA-2:DMPC disks show hysteresis at any scan rate, indicating intrinsic thermodynamic irreversibility of the transition (Fig. 3 *A*). Furthermore, the CD melting curves shift to lower temperatures upon reduction in the heating rate from 1.33 to 0.193 K/min (from the apparent T_m = 84°C to 75°C). Such scan rate dependence, which was also observed in apoA-1:DMPC (Surewicz et al., 1986; Fang et al., 2003) and apoC-1:DMPC disks (Gursky et al., 2002; Mehta et al., 2003a), is characteristic of thermodynamically irreversible reactions with high activation energy (Sanchez-Ruiz et al., 1988). Slowing down the scan rate also leads to a reduction in the CD amplitude in the cooling curves below 80°C (Fig. 3 *A*), which may result from protein aggregation upon prolonged exposure to high temperatures.

Changes in the 90° light scattering observed during heating and cooling of the apoA-2:DMPC complexes correlate with the CD changes (Fig. 3, *A* and *B*). The negative slope in the heating and cooling curves in Fig. 3 *B* is independent of the scan rate and results from the temperature dependence of the refractive index. At high temperatures, a steep increase in the light scattering is observed, suggesting an increase in the particle size and/or refractive index due to disk fusion. A similar heat-induced increase in the apoC-1:DMPC lipoprotein size due to fusion was observed by turbidity (Gursky et al., 2002; Mehta et al., 2003a). In these experiments, disk fusion coincided with the apoC-1 unfolding; in contrast, comparison of the corresponding CD and light-scattering data in Fig. 3, *A* and *B*, suggests that the apoA-2 unfolding precedes lipoprotein fusion. For example, the CD curve recorded at 1.33 K/min is sigmoidal and reaches a plateau at high temperatures, suggesting that the unfolding transition is complete at 99°C, yet the light-scattering curve recorded in

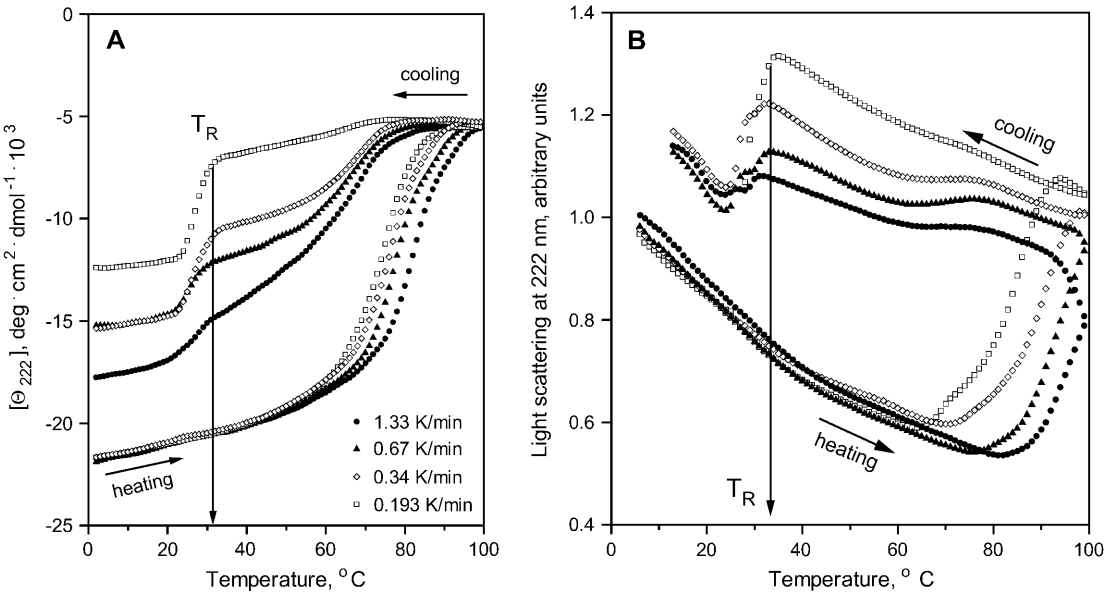

FIGURE 3 Scan-rate effects on far-UV CD and light-scattering melting curves of apoA-2:DMPC disks. The CD (*A*) and light-scattering melting curves (*B*) were recorded simultaneously at 222 nm during sample heating and cooling at various scan rates from 1.33 to 0.193 K/h. The directions of temperature changes are indicated. The temperature T_R of the protein-lipid complex reconstitution upon cooling is shown by arrow.

the same experiment does not reach a plateau, and the signal continues to increase upon cooling from 99°C (Fig. 3, *A* and *B*, *solid circles*). Also, the onset of the light-scattering transition during heating at 1.33 K/min is observed above 80°C, ~10°C higher than the onset of the corresponding CD transition. This suggests that the apoA-2:DMPC disk-to-vesicle fusion is a multiphase reaction that is triggered by the apoA-2 unfolding at an early stage.

Similar to the CD data, the light-scattering heating curves of the apoA-2:DMPC disks shift to lower temperatures at slower scan rates, indicating high activation energy for the disk fusion. Slowing the heating rate also leads to a larger increase in the light scattering at high temperatures, suggesting that prolonged exposure to high temperatures leads to formation of larger vesicles. This is consistent with the EM data showing formation of large liposomes upon increasing the time and/or temperature of the sample incubation (Fig. 2 *C*).

The light-scattering cooling curves recorded at faster rates (1.33–0.34 K/min) suggest a small gradual reduction in the particle size below 80°C that parallels the CD changes at these temperatures (Fig. 3, *A* and *B*). Further cooling leads to a steep reduction in the light scattering (and thus in the particle size) between 34 and 24°C. The onset of this transition at various scan rates is observed at $T_R = 32$–34°C, similar to T_R inferred from the CD data. Taken together, these data indicate that heating of the apoA-2:DMPC disks to 99°C leads to protein unfolding and disk-to-vesicle fusion; consecutive cooling leads to a gradual reduction in the vesicle size and partial protein refolding, followed by formation of smaller protein-containing vesicles and additional helical refolding at 34–24°C. Thus, the heating and cooling curves in Fig. 5, *A* and *B*, show a correlation between the protein folding/unfolding and the changes in the particle morphology.

To quantitate the unfolding kinetics of apoA-2 on DMPC, we monitored the time course of the protein unfolding. The unfolding was triggered at $t = 0$ by a temperature-jump from 25°C to 75–95°C and was monitored by CD at 222 nm (Fig. 4). The $\Theta_{222}(t)$ data show slow unfolding on a timescale of 10^2–10^3 s (as compared to 10^{-8}–10^{-10} s for the helix-to-coil transition in solution; Yang and Gruebele, 2003), implicating high free-energy barrier ΔG^*. The unfolding rate increases at higher temperatures, indicating high enthalpic contribution ΔH^* to this barrier. To determine the activation energy (enthalpy) $E_a \cong \Delta H^*$, the $\Theta_{222}(t)$ data were fitted by exponentials (Fig. 4 *A*, *solid lines*). The T-jump data to 95°C are well approximated by a single exponential, yet two exponents are required to fit the data at 75–90°C, suggesting two kinetic phases. Arrhenius plots for these phases are linear and intercept near 100°C (Fig. 4 *B*), thus one exponent adequately fits the data at 100°C. The slopes of the Arrhenius plots suggest activation energy $E_{a,fast} = 22 \pm 5$ kcal/mol for the fast phase and $E_{a,slow} = 60 \pm 7$ kcal/mol for the slow phase.

The melting and kinetic CD data in Figs. 3 and 4 are invariant with the changes in the disk concentration in the range explored, thus the unfolding rate is not significantly affected by the lipoprotein concentration. Importantly, our studies of DMPC disks with apoA-1 (unpublished data) and apoC-1 (Mehta et al., 2003a) clearly show that variations in the disk diameter from 9 to 18 nm have no significant effect on the disk stability. Thus, the size heterogeneity of the

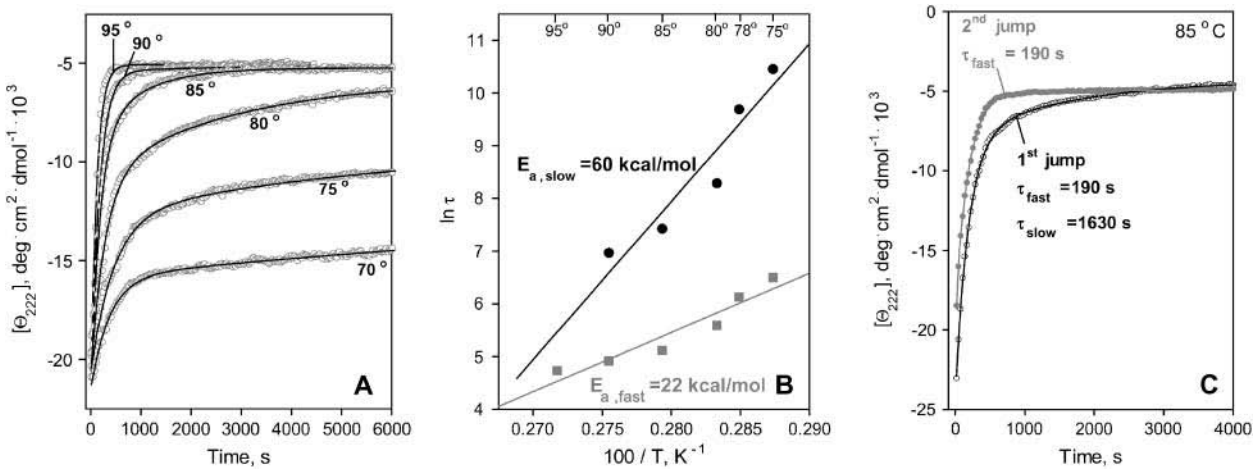

FIGURE 4 Thermal denaturation kinetics of apoA-2:DMPC complexes. (*A*) CD data $\Theta_{222}(t)$ recorded at 222 nm of intact disks in T-jumps from 25°C to higher temperatures (indicated on the *lines*); solid lines show bi-exponential data fitting. (*B*) Arrhenius plots, ln τ versus $1/T$, obtained from the bi-exponential fitting of the data in *A*; the activation energies E_a determined from the slopes of the Arrhenius plots are shown. (*C*) CD data $\Theta_{222}(t)$ recorded from the same sample in two consecutive T-jumps from 25 to 85°C as described in the text. The data in the first jump (initial state is intact disks) are fitted by a bi-exponential (shown by *solid line*), and the two exponential relaxation times are indicated. The data in the second jump (initial state is a mixture of lipid-poor and vesicle-bound apoA-2) is fitted by a mono-exponential (*solid line*).

apoA-2:DMPC disks may not account for their multiphase unfolding kinetics.

To probe the origin of the two kinetic phases, we recorded $\Theta_{222}(t)$ data from the same apoA-2:DMPC sample in repetitive T-jumps. Fig. 4 *C* shows the data recorded in the first and second jump from 25 to 85°C. Once protein unfolding reached completion in the first jump, the sample was cooled and incubated at 25°C for 1000 s, which was sufficient for completion of the helical refolding (as indicated by flattening of the $\Theta_{222}(t)$) but not for the disk reconstitution (as indicated by DSC, EM, and gel electrophoresis). Afterwards, the second jump from 25 to 85°C was performed, etc. Thus, the initial state in the first jump was intact disks, and in the second jump it was a mixture of protein-containing vesicles and lipid-poor protein. The $\Theta_{222}(t)$ data recorded in the second and consecutive jumps were similar, indicating faster unfolding than in the first jump (Fig. 4 *C*). Data fitting suggests that, in contrast to the double-exponential kinetics in the first jump ($\tau_{fast} = 190$ s, $\tau_{slow} = 1630$ s), the data in the second jump are well approximated by a single exponent with a relaxation time $\tau = 190$ s, which is similar to τ_{fast}. Repetitive jumps to other temperatures yielded similar results. Thus, the fast unfolding phase is observed in disks and in the mixture of lipid-poor and vesicle-bound apoA-2, whereas the slow unfolding phase is observed in disks only. Similarly, repetitive T-jumps with DMPC disks containing apoA-1 and apoC-1 show faster unfolding in the second and consecutive jumps (data not shown). Consequently, lipid-poor and vesicle-bound apolipoproteins have lower kinetic stability than the disks.

Chemical unfolding kinetics of the apoA-2:DMPC disks was probed in denaturant-jump experiments. The time course of the protein unfolding, which was triggered by a rapid increase in the Gdm HCl concentration from 0 to 1–6 M, was monitored by CD at 222 nm (Fig. 5). The $\Theta_{222}(t)$ data show a rapid signal loss at any Gdm HCl concentration,

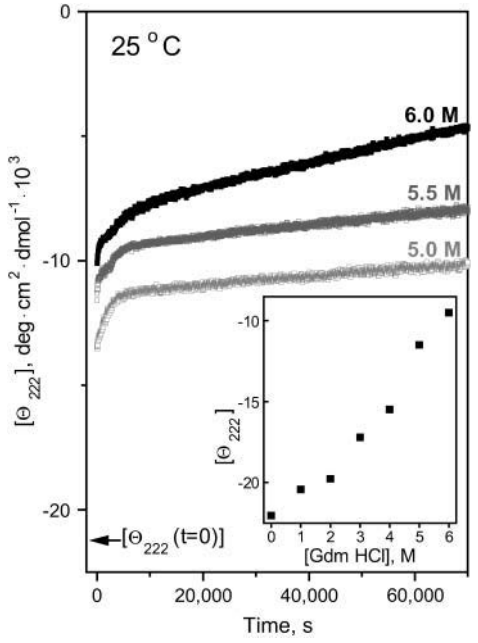

FIGURE 5 Chemical denaturation kinetics of apoA-2:DMPC disks. The time course of the protein unfolding, which was triggered at $t = 0$ by increasing Gdm HCl concentration from 0 M to a final value indicated on the lines, was monitored by CD at 222 nm. Arrow shows the value of $[\Theta_{222}]$ in 0 M Gdm HCl. (*Inset*) $[\Theta_{222}]$ measured during the initial 30-s exposure of intact disks to Gdm HCl.

indicating fast unfolding within the dead-time of the experiment (30 s), which precludes its quantitative analysis; the amplitude of this rapid phase increases with increasing denaturant concentration (Fig. 5, *inset*). In addition, slower multiphase unfolding is detected at higher denaturant concentrations. Similar multiphase kinetics of the Gdm-induced unfolding was observed in apoA-1:DMPC disks (Reijngoud and Phillips, 1982) and in apoC-1 disks (unpublished data). The EM data show that disk incubation in high Gdm HCl concentrations leads to a small but significant increase in the particle diameter (Fig. 2 *D*). In summary, chemical denaturation of discoidal lipoproteins is a complex multiphase transition whose kinetics is distinctly different from that of the thermal denaturation; similar to thermal denaturation, chemical denaturation involves protein unfolding/dissociation (Reijngoud and Phillips, 1982) and lipoprotein fusion (Fig. 2 *D*).

Comparison with apoA-1 and apoC-1

To assess the relative stability of the DMPC complexes with various human apolipoproteins, we used DSC, CD, and light scattering to monitor heat denaturation of similar-size DMPC disks with apoA-1, apoA-2, or apoC-1 under otherwise identical conditions. Fig. 6, *A–C*, show these data for apoA-1- and apoA-2-containing disks. Similar CD and turbidity data of apoC-1:DMPC disks were reported earlier (Gursky et al., 2002), and the DSC data show only the lipid phase transition but lack the high-temperature peak because of the low unfolding enthalpy of this small protein. The DSC data recorded of apoA-1- and apoA-2-containing disks upon heating at 90 K/h show that the unfolding/dissociation of apoA-1 is centered at 91°C, ~7°C higher than the apoA-2 transition (Fig. 6 *A*). This agrees with the trend observed by CD and light scattering; for example, the heating curves recorded at 11 K/h show that apoA-1:DMPC disks undergo protein unfolding and lipoprotein fusion at higher temperatures than similar disks containing apoA-2 (Fig. 6, *B* and *C*) or apoC-1 (Gursky et al., 2002). Furthermore, the amplitude of the light-scattering changes in apoA-1:DMPC complexes is significantly smaller than that in apoA-2 complexes, suggesting that apoA-1 inhibits disk fusion more effectively than apoA-2. This is confirmed by EM showing that similar thermal treatment leads to a significantly larger increase in the diameter of the apoA-2-containing complexes (Fig. 2, *B* and *C*) than in similar complexes with apoA-1 (data not shown). Taken together, our DSC, CD, light-scattering, and EM data clearly show that apoA-1:DMPC disks undergo heat denaturation at higher temperatures and are less prone to fusion than similar disks with apoA-2.

To compare the activation energy E_a of disk denaturation for different proteins, we recorded T-jump CD data of apoA-1:DMPC disks (Fig. 7 *A*). These data were well approximated by mono-exponential functions, and the Arrhenius analysis yielded the activation energy $E_a = 50 \pm 5$ kcal/mol, consistent with our estimate based on the scan rate effects on the melting data (Fang et al., 2003). This value of E_a is comparable to the activation energy for the slow phase of apoA-2:DMPC disk denaturation (Fig. 4 *B*).

To assess relative kinetic stability of the DMPC disks containing various apolipoproteins, we compared the rates of their thermal unfolding. The CD data of the apoA-1-, apoA-2-, and apoC-1-containing disks recorded in a T-jump from 25 to 85°C indicate that the unfolding is slowest for apoA-1 and fastest for apoC-1 (Fig. 7 *B*); T-jumps to other temperatures show a similar trend. A similar rank order is suggested by the comparison of the melting temperatures assessed

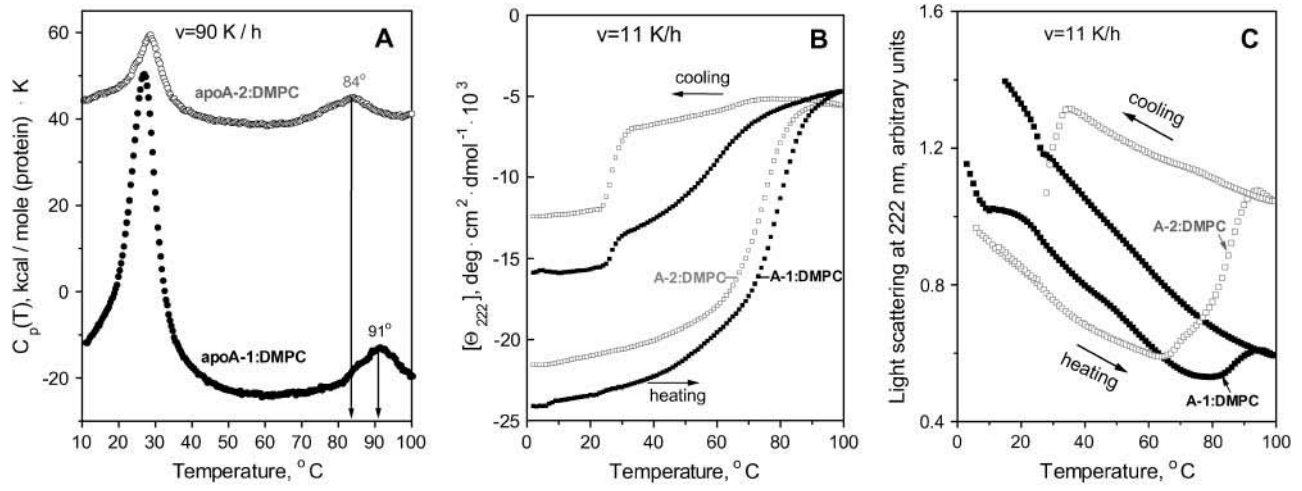

FIGURE 6 Thermal unfolding of apoA-1 and apoA-2 in DMPC complexes. (*A*) Excess heat capacity $C_p(T)$ of DMPC disks with apoA-1 (●) and apoA-2 (○) recorded by DSC during heating at 90 K/h. The data are shifted along the *y* axis to avoid overlap; the peak positions of the protein unfolding transition are indicated. (*B*) CD melting curves $\Theta_{222}(T)$ and (*C*) light-scattering data of the disks recorded simultaneously during heating and cooling at 0.193 K/min (11 K/h). Standard buffer solutions containing 0.7 mg/ml protein (in DSC) and 20 μg/ml protein (in CD and light-scattering experiments) were used.

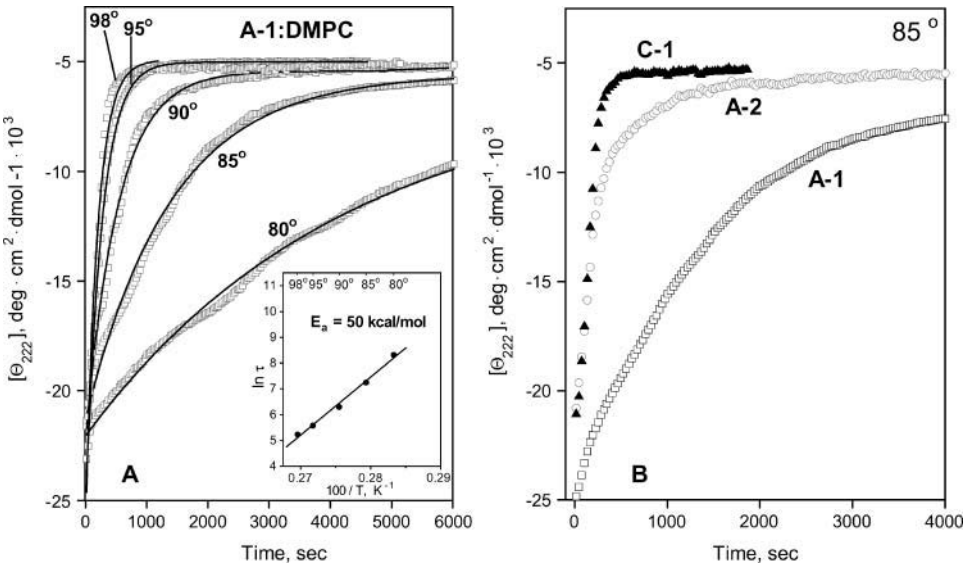

FIGURE 7 Thermal denaturation kinetics of apoA-1:DMPC complexes compared to similar complexes with apoA-2 and apoC-1. (*A*) CD data at 222 nm recorded in T-jumps with disks from 25°C to higher temperatures (indicated on the *lines*); solid lines show mono-exponential data fitting. (*Inset*) Arrhenius plot, ln τ versus $1/T$, yields the activation energy $E_a = 50 \pm 5$ kcal/mol. (*B*) Thermal unfolding kinetics of DMPC disks containing various apolipoproteins. CD data $\Theta_{222}(t)$ of the disk solutions containing apoA-1 (□), apoA-2 (○), and apoC-1 (▲) under otherwise identical conditions were recorded in a T-jump from 25 to 85°C; jumps to other temperatures (65–95°C) reveal a similar rank order, with apoA-1 showing the slowest and apoC-1 the fastest unfolding.

by DSC, CD, and light scattering in this (Fig. 6, *A–C*) and earlier studies (Gursky et al., 2002; Fang et al., 2003). For example, the apparent melting temperatures inferred from the CD data recorded at 80 K/h are $T_{m,A-1} = 91$°C, $T_{m,A-2} = 84$°C, and $T_{m,C-1} = 72$°C. In summary, both the kinetic (Fig. 7 *B*) and the melting data recorded by CD, light scattering, and DSC (Fig. 6; Gursky et al., 2002) indicate similar rank order for the DMPC disk stability, apoA-1 > apoA-2 > apoC-1.

DISCUSSION

The results of this work, together with the earlier studies of apoA-1:DMPC (Reijngoud and Phillips, 1982; Fang et al., 2003) and apoC-1:DMPC disks (Gursky et al., 2002; Mehta et al., 2003a), show that the heat- and denaturant-induced transitions in discoidal lipoproteins are kinetically controlled reactions that involve protein unfolding, dissociation, and lipoprotein fusion. The fastest unfolding phase in apoA-2:DMPC disks was detected during the dead-time in the denaturant-jump experiments ($\tau < 30$ s, Fig. 5); a similar fast phase in apoA-1:DMPC disks was attributed to the reversible unfolding of the lipoprotein-anchored protein (Reijngoud and Phillips, 1982). The slower irreversible phases in the Gdm denaturation have been shown to involve protein dissociation (Reijngoud and Phillips, 1982); our EM data suggest disk fusion at this stage (Fig. 2 *D*). In contrast to the denaturant-jumps, T-jumps with apoA-2:DMPC (Fig. 4 *A*), apoA-1:DMPC (Fig. 7 *A*), and apoC-1:DMPC disks (Gursky et al., 2002) do not show a rapid reversible unfolding of the disk-anchored protein; instead, they exhibit relatively slow protein unfolding, dissociation, and disk fusion (Fig. 2). Comparison of the timescales of the protein unfolding on the disks, 10^2–10^4 s (Fig. 4), with the helix-to-coil transition in solution, 10^{-8}–10^{-10} s (Yang and Gruebele, 2003), shows that protein-lipid association decelerates the unfolding by at least 10 orders of magnitude, implicating high kinetic barriers. Taken together, our results indicate that thermal and chemical denaturation of discoidal HDL proceed via distinct pathways, yet they both involve high kinetic barriers that arise from the protein dissociation and disk fusion.

Earlier CD and turbidity studies of apoC-1:DMPC disks suggested that protein unfolding is tightly coupled to disk fusion (Gursky et al., 2002); however, correlation of the CD and 90° light-scattering data in Fig. 3, *A* and *B*, indicates that, in apoA-2:DMPC complexes, protein unfolding precedes fusion, suggesting only loose coupling. Furthermore, the bi-exponential heat-unfolding kinetics observed in apoA-2:DMPC disks (Fig. 4), which contrasts with the mono-exponential unfolding kinetics of apoC-1:DMPC and apoA-1:DMPC disks, may possibly relate to the dimeric nature of human apoA-2. Interestingly, the activation energy $E_a = 60 \pm 8$ kcal/mol of the slow heat-unfolding phase in apoA-2:DMPC disks (Fig. 4 *B*) is comparable to that observed in apoA-1:DMPC disks (Fig. 6 *B*). Since the major enthalpic contribution $\Delta H^* \cong E_a$ to the free energy barrier $\Delta G^* = \Delta H^* - T\Delta S^*$ for the disk denaturation may arise from the transient disruption of the predominantly hydrophobic protein-lipid interactions, similar values of E_a may reflect similar combined hydrophobic surfaces in the amphipathic α-helices in apoA-1 and apoA-2 that are comprised of ~50 amino acids in the lipid-bound state of these proteins.

A surprising result is the rank order of the kinetic disk stability $\Delta G^* \sim \ln \tau$ that is evident from the timescales of the heat denaturation, apoA-1 > apoA-2 > apoC-1 (Fig. 7 *B*), and from the apparent melting temperatures determined by CD, light scattering, and DSC, $T_{m,apoA-1} > T_{m,apoA-2} > T_{m,apoC-1}$ (Fig. 6; Gursky et al., 2002).This ranking suggests that the disk stability correlates with the protein size rather than hydrophobicity. Further support for this hypothesis

comes from a large reduction in the apparent T_m and faster thermal unfolding observed upon disulfide reduction in apoA-2:DMPC disks (data not shown), which is consistent with the report that apoA-2 on the disks is less stable in monomeric than in dimeric form (Lund-Katz et al., 1996).

Correlation between the protein size and disk stability may result from enthalpic and/or entropic effects. The former may reflect the relative ease with which a smaller protein with fewer lipid-binding helices can dissociate from the disk as compared to a larger protein with multiple, possibly cooperative lipid binding sites. The entropic effect may result from the contribution of the cratic (mixing) entropy of protein dissolution to the entropy of disk denaturation. In our model, cratic entropy reflects the fact that multiple protein molecules are held together on the disk (low-entropy state) but dissociate in solution (high-entropy state). Cratic entropy for dissociation of a single polypeptide is lower than that of its fragments; similarly, it is lower for larger proteins. As a result, disks containing larger proteins have lower unfavorable entropic contribution $T\Delta S^*$ to their kinetic stability $\Delta G^* = \Delta H^* - T\Delta S^*$, leading to higher stability.

Interestingly, the light-scattering melting curves show a smaller heat-induced increase in the particle size for apoA-1 than apoA-2-containing disks (Fig. 6 *C*). This is confirmed by EM, showing that similar thermal treatment leads to more extensive fusion of DMPC complexes with apoA-2 (Fig. 2) than those with apoA-1 (data not shown). These results suggest that apoA-1 is a more efficient inhibitor of disk fusion than apoA-2. This may possibly relate to the ability of the central part of apoA-1, but not apoA-2, to be displaced from HDL (Durbin and Jonas, 1997), with the N- and C-terminal segments of apoA-1 anchored in the lipoprotein and thereby precluding its fusion.

Lipoprotein fusion observed in our work is accelerated under denaturing conditions (Figs. 4, 6, and 7) that promote protein dissociation, thereby creating a mismatch between the depleted particle surface and its core that leads to fusion. Under physiological conditions, spontaneous lipoprotein fusion is very slow due to high kinetic barriers. These barriers can be overcome by proteolytic or lipolytic enzymes such as LCAT, phospholipid transfer protein, or cholesterol ester transfer protein. These enzymes deplete the polar HDL surface of the proteins or phospholipids and/or increase the apolar lipid core, thereby creating a mismatch between the particle surface and its core (Clay et al., 2000; Rye and Barter, 2004; Jayaraman et al., 2004, and references therein). Thus, the observed difference between the effects of apoA-1 and apoA-2 on the disk fusion may be important for the in vivo formation of LpA-1/A-2 which is proposed to involve LCAT-mediated fusion of small LpA-1 with LpA-2 (Clay et al., 2000). Since only LpA-1, but not LpA-2, provide substrates for LCAT, formation of LpA-1/A-2 may be facilitated by the relative ease of spontaneous LpA-2 fusion. Also, since apolipoprotein ability to prevent HDL fusion with the cell membrane is proposed to play a key role in the receptor-mediated selective cholesterol uptake from HDL (Thuahnai et al., 2001), different antifusogenic action of apoA-1 and apoA-2 may contribute to the observed differences in the receptor-mediated lipid uptake from LpA-1 and LpA-1/A-2 (Blanco-Vaca et al., 2001; De Beer et al., 2001; Rinninger et al., 2003). In addition, comparative studies of antifusogenic effects of apolipoproteins, such as this work, may help to develop apolipoprotein-based peptides with optimized antiviral properties (Srinivas et al., 1991).

Surprisingly, the rank order for the disk stability indicated by our DSC, CD, and light-scattering data (Figs. 6 and 7 *B*) differs from the stability ranking apoA-2 > apoA-1 that is inferred for plasma spherical HDL and is attributed to deeper penetration of the more hydrophobic apoA-2 α-helices in the lipid milieu (Brasseur et al., 1992; Forte et al., 1995). This suggests different modes of lipid-protein interactions in plasma spherical and model discoidal HDL, which may result from different chemical composition and/or geometry of these particles. Thus, although the general mechanism of kinetic stabilization is similar for HDL disks and spheres, the molecular determinants for their stability are significantly different.

Another unanticipated result is the observation of a repeatable lipoprotein transition that is thermodynamically irreversible. The high-temperature transition in apoA-2:DMPC disks (*solid circles*, Fig. 1, *A* and *B*; *curve 1*, Fig. 1 *C*) is invariant in repetitive CD and DSC scans (*curves 2–4*, Fig. 1 *C*), yet it shows hysteresis and scan rate effects characteristic of thermodynamically irreversible reactions, as indicated by the CD and light-scattering data in Fig. 3, *A* and *B*. Moreover, protein unfolding and dissociation in this transition lead to thermodynamically irreversible disk fusion, as indicated by the DSC, EM, and gel electrophoresis data (Fig. 1 *C*, *curves 2–4*; Fig. 2, *B* and *C*; Fig. 2 *E*, *lanes 5–10*). This exemplifies that the correct criterion for thermodynamic reversibility is the absence of scan rate effects and hysteresis rather than the repeatability of a transition.

In apoA-2:DMPC complexes, the repeatability of the high-temperature transition that involves unfolding of lipidated apoA-2 (Fig. 2, *curves 1–4*) indicates that this transition is invariant regardless of the nature of the complex (intact disks in the first scan or a mixture of vesicle-bound and monomolecular lipid-poor apoA-2 in the second and consecutive scans). This suggests that the cooperativity unit in this transition comprises a single copy of lipidated apoA-2 rather than the entire lipoprotein. Repetitive T-jumps with DMPC complexes containing apoA-1, apoC-1, or apoA-2 show that the protein unfolding in the first jump is slower than that in consecutive jumps (Fig. 4 *C*), indicating higher kinetic stability of the disks as compared to lipid-poor and vesicle-bound protein. In summary, our results suggest that lipid-bound apolipoproteins in discoidal, vesicular, and in lipid-poor states are stabilized by kinetic barriers, and that these barriers are higher for the disks. This extends the results of our kinetic studies of model discoidal (Gursky

et al., 2002; Mehta et al., 2003a; Fang et al., 2003) and plasma spherical HDL (Mehta et al., 2003b, Jayaraman et al., 2004), and LDL (Jayaraman et al., 2005), and substantiates the hypothesis that the kinetic mechanism provides a universal natural strategy for stabilization of diverse macromolecular systems (Plaza del Pino et al., 2000), including lipid-protein complexes.

We thank Cheryl England and Michael Gigliotti for apolipoprotein isolation and purification, and Sangeeta Benjwal and Madhumita Guha for general help.

This work was supported by National Institutes of Health grant No. GM67260 to O. G. The CD spectroscopy, calorimetry, electron microscopy, and biochemistry core facilities are supported, in part, by National Institutes of Health grant No. HL26355 (D. Atkinson, Program Director).

REFERENCES

Barter, P. J., and K. A. Rye. 1996. High density lipoproteins and coronary heart disease. *Atherosclerosis.* 121:1–12.

Blanco-Vaca, F., J. C. Escola-Gil, J. M. Martin-Campos, and J. Julve. 2001. Role of apoA-II in lipid metabolism and atherosclerosis: advances in the study of an enigmatic protein. *J. Lipid Res.* 42:1727–1739.

Boucher, J., T. A. Ramsamy, S. Braschi, D. Sahoo, T. A. Neville, and D. L. Sparks. 2004. Apolipoprotein A-II regulates HDL stability and affects hepatic lipase association and activity. *J. Lipid Res.* 45:849–858.

Brasseur, R., L. Lins, B. Vanloo, J. M. Ruysschaert, and M. Rosseneu. 1992. Molecular modeling of the amphipathic helices of the plasma apolipoproteins. *Proteins.* 13:246–257.

Calabresi, L., A. Lucchini, G. Vecchio, C. R. Sirtori, and G. Franceschini. 1996. Human apolipoprotein A-II inhibits the formation of pre-beta high density lipoproteins. *Biochim. Biophys. Acta.* 1304:32–42.

Chapman, D. 1975. Phase transitions and fluidity characteristics of lipids and cell membranes. *Q. Rev. Biophys.* 8:185–235.

Cheung, M. C., and J. J. Albers. 1984. Characterization of lipoprotein particles isolated by immunoaffinity chromatography: particles containing A-I and A-II and particles containing A-I but no A-II. *J. Biol. Chem.* 259:12201–12209.

Cheung, M. C., A. C. Wolf, R. H. Knopp, and D. M. Foster. 1992. Protein transfer between A-I-containing lipoprotein subpopulations: evidence of non-transferable A-I in particles with A-II. *Biochim. Biophys. Acta.* 1165:68–77.

Clay, M. A., D. H. Pyle, K. A. Rye, and P. J. Barter. 2000. Formation of spherical, reconstituted high density lipoproteins containing both apolipoproteins A-I and A-II is mediated by lecithin:cholesterol acyltransferase. *J. Biol. Chem.* 275:9019–9025.

Davidson, W. S., K. L. Gillotte, S. Lund-Katz, W. J. Johnson, G. H. Rothblat, and M. C. Phillips. 1995. The effect of high density lipoprotein phospholipid acyl chain composition on the efflux of cellular free cholesterol. *J. Biol. Chem.* 270:5882–5890.

De Beer, M. C., D. M. Durbin, L. Cai, N. Mirocha, A. Jonas, N. R. Webb, F. C. de Beer, and D. R. van Der Westhuyzen. 2001. Apolipoprotein A-II modulates the binding and selective lipid uptake of reconstituted high density lipoprotein by scavenger receptor BI. *J. Biol. Chem.* 276:15832–15839.

Donovan, J. M., G. B. Benedek, and M. C. Carey. 1987. Self-association of human apolipoproteins A-I and A-II and interactions of apolipoprotein A-I with bile salts: quasi-elastic light scattering studies. *Biochemistry.* 26:8116–8125.

Durbin, D. M., and A. Jonas. 1997. The effect of apolipoprotein A-II on the structure and function of apolipoprotein A-I in a homogeneous reconstituted high density lipoprotein particle. *J. Biol. Chem.* 272:31333–31339.

Epand, R. M. 1982. The apparent preferential interactions of human plasma high-density apolipoprotein A-1 with gel-state phospholipids. *Biochim. Biophys. Acta.* 712:146–151.

Fang, Y., O. Gursky, and D. Atkinson. 2003. Lipid binding studies of human apolipoprotein A-1 and its terminally truncated mutants. *Biochemistry.* 42:13260–13268.

Fielding, C. J., and P. E. Fielding. 1995. Molecular physiology of reverse cholesterol transport. *J. Lipid Res.* 36:211–228.

Forte, T. M., J. K. Bielicki, R. Goth-Goldstein, J. Selmek, and M. R. McCall. 1995. Recruitment of cell phospholipids and cholesterol by apolipoproteins A-II and A-I: formation of nascent apolipoprotein-specific HDL that differ in size, phospholipid composition, and reactivity with LCAT. *J. Lipid Res.* 36:148–157.

Gursky, O., and D. Atkinson. 1996a. I. Thermal unfolding of human high-density apolipoprotein A-1: implications for a lipid-free molten globular state. *Proc. Natl. Acad. Sci. USA.* 93:2991–2995.

Gursky, O., and D. Atkinson. 1996b. II. High- and low-temperature unfolding of human high-density apolipoprotein A-2. *Protein Sci.* 5:1874–1882.

Gursky, O., Ranjana, and D. L. Gantz. 2002. Complex of human apolipoprotein C-1 with phospholipid: thermodynamic or kinetic stability? *Biochemistry.* 41:7373–7384.

Hedrick, C. C., and A. J. Lusis. 1994. Apolipoprotein A-II, a protein in search of a function. *Can. J. Cardiol.* 10:453–459.

Hedrick, C. C., L. W. Castellani, H. Wong, and A. J. Lusis. 2001. In vivo interactions of apoA-II, apoA-I, and hepatic lipase contributing to HDL structure and antiatherogenic functions. *J. Lipid Res.* 42:563–570.

Jayaraman, S., D. L. Gantz, and O. Gursky. 2004. Poly(ethylene glycol)-induced fusion and destabilization of human high-density lipoproteins. *Biochemistry.* 43:5520–5531.

Jayaraman, S., D. L. Gantz, and O. Gursky. 2005. Structural basis for thermal stability of human low-density lipoprotein. *Biochemistry.* 44:3965–3971.

Jonas, A. 1986. Reconstitution of high-density lipoproteins. *Methods Enzymol.* 128:553–582.

Kumar, M. S., M. Carson, M. M. Hussain, and H. M. Murthy. 2002. Structures of apolipoprotein A-II and a lipid-surrogate complex provide insights into apolipoprotein-lipid interactions. *Biochemistry.* 41:11681–11981.

Labeur, C., G. Lambert, T. Van Cauteren, N. Duverger, B. Vanloo, J. Chambaz, J. Vandekerckhove, G. Castro, and M. Rosseneu. 1998. Displacement of apo A-I from HDL by apo A-II or its C-terminal helix promotes the formation of pre-β1 migrating particles and decreases LCAT activation. *Atherosclerosis.* 139:351–362.

Lund-Katz, S., L. Liu, S. T. Thuahnai, and M. C. Phillips. 2003. High density lipoprotein structure. *Front. Biosci.* 8:d1044–d1054.

Lund-Katz, S., Y. M. Murley, E. Yon, K. L. Gillotte, and W. S. Davidson. 1996. Comparison of the structural and functional effects of monomeric and dimeric human apolipoprotein A-II in high density lipoprotein particles. *Lipids.* 31:1107–1113.

Luo, C. C., W. H. Li, M. N. Moore, and L. Chan. 1986. Structure and evolution of the apolipoprotein multigene family. *J. Mol. Biol.* 187:325–340.

Mao, D., and B. A. Wallace. 1984. Differential light scattering and absorption flattening optical effects are minimal in the circular dichroism spectra of small unilamellar vesicles. *Biochemistry.* 23:2667–2673.

Massey, J. B., A. M. Gotto, Jr., and H. J. Pownall. 1981. Thermodynamics of lipid-protein interactions: interaction of apolipoprotein A-II from human plasma high-density lipoproteins with dimyristoyl phosphatidylcholine. *Biochemistry.* 20:1575–1584.

Mehta, R., D. L. Gantz, and O. Gursky. 2003a. I. Effects of mutations in apolipoprotein C-1 on the reconstitution and kinetic stability of discoidal lipoproteins. *Biochemistry.* 42:4751–4758.

Mehta, R., D. L. Gantz, and O. Gursky. 2003b. II. Human plasma high-density lipoproteins are stabilized by kinetic factors J. *Mol. Biol.* 328:183–192.

Nichols, A. V., E. L. Gong, P. J. Blanche, T. M. Forte, and D. W. Anderson. 1976. Effects of guanidine hydrochloride on human plasma high density lipoproteins. *Biochim. Biophys. Acta.* 446:226–239.

Osborne, J. C., Jr., G. Palumbo, H. B. Brewer, Jr., and H. Edelhoch. 1976. The thermodynamics of the self-association of the reduced and carboxymethylated form of apoA-II from the human high density lipoprotein complex. *Biochemistry.* 15:317–320.

Pastier, D., S. Dugue, E. Boisfer, V. Atger, N. Q. Tran, A. van Tol, M. J. Chapman, J. Chambaz, P. M. Laplaud, and A. D. Kalopissis. 2001. Apolipoprotein A-II/A-I ratio is a key determinant in vivo of HDL concentration and formation of pre-β HDL containing apolipoprotein A-II. *Biochemistry.* 40:12243–12253.

Plaza del Pino, I. M., B. Ibarra-Molero, and J. M. Sanchez-Ruiz. 2000. Lower kinetic limit to protein thermal stability: a proposal regarding protein stability in vivo and its relation with misfolding diseases. *Proteins.* 40:58–70.

Pussinen, P. J., M. Jauhiainen, and C. Ehnholm. 1997. ApoA-II/apoA-I molar ratio in the HDL particle influences phospholipid transfer protein-mediated HDL interconversion. *J. Lipid Res.* 38:12–21.

Reijngoud, D.-J., and M. C. Phillips. 1982. Mechanism of dissociation of human apolipoprotein A-1 from complexes with DMPC as studied by guanidine hydrochloride denaturation. *Biochemistry.* 21:2969–2976.

Remaley, A. T., J. A. Stonik, S. J. Demosky, E. B. Neufeld, A. V. Bocharov, T. G. Vishnyakova, T. L. Eggerman, A. P. Patterson, N. J. Duverger, S. Santamarina-Fojo, and H. B. Brewer, Jr. 2001. Apolipoprotein specificity for lipid efflux by the human ABCAI transporter. *Biochem. Biophys. Res. Commun.* 280:818–823.

Rinninger, F., M. Brundert, R. M. Budzinski, J. C. Fruchart, H. Greten, and G. R. Castro. 2003. Scavenger receptor BI (SR-BI) mediates a higher selective cholesteryl ester uptake from LpA-I compared with LpA-I, A-II lipoprotein particles. *Atherosclerosis.* 166:31–40.

Ritter, M. C., and A. M. Scanu. 1979. Apolipoprotein A-II and structure of human serum high density lipoproteins. An approach by reassembly techniques. *J. Biol. Chem.* 254:2517–2525.

Rye, K. A., K. Wee, L. K. Curtiss, D. J. Bonnet, and P. J. Barter. 2003. Apolipoprotein A-II inhibits high density lipoprotein remodeling and lipid-poor apolipoprotein A-I formation. *J. Biol. Chem.* 278:22530–22536.

Rye, K. A., and P. J. Barter. 2004. Formation and metabolism of pre-β-migrating, lipid-poor apolipoprotein A-I. *Arterioscler. Thromb. Vasc. Biol.* 24:421–428.

Sanchez-Ruiz, J. M., J. L. Lopez-Lacomba, M. Cortijo, and P. L. Mateo. 1988. Differential scanning calorimetry of irreversible thermal denaturation of thermolysin. *Biochemistry.* 27:1648–1652.

Schumaker, V. N., and D. L. Puppione. 1986. Sequential flotation ultracentrifugation. *Methods Enzymol.* 128:155–170.

Segrest, J. P., M. K. Jones, H. De Loof, C. G. Brouillette, Y. V. Venkatachalapathi, and G. M. Anantharamaiah. 1992. The amphipathic helix in the exchangeable apolipoproteins: a review of secondary structure and function. *J. Lipid Res.* 33:141–166.

Sparks, D. L., P. G. Frank, S. Braschi, T. A. M. Neville, and Y. L. Marcel. 1999. Effect of apolipoprotein A-I lipidation on the formation and function of pre-β and α-migrating LpA-I particles. *Biochemistry.* 38:1727–1735.

Srinivas, R. V., Y. V. Venkatachalapathi, Z. Rui, R. J. Owens, K. B. Gupta, S. K. Srinivas, G. M. Anantharamaiah, J. P. Segrest, and R. W. Compans. 1991. Inhibition of virus-induced cell fusion by apolipoprotein A-I and its amphipathic peptide analogs. *J. Cell. Biochem.* 45:224–237.

Surewicz, W. K., R. M. Epand, H. J. Pownall, and S.-W. Hui. 1986. Human apolipoprotein A-I forms thermally stable complexes with anionic but not with zwitterionic phospholipids. *J. Biol. Chem.* 34:16191–16197.

Swaney, J. B., and K. O'Brien. 1978. Cross-linking studies of the self-association properties of apo-A-I and apo-A-II from human high density lipoprotein. *J. Biol. Chem.* 253:7069–7077.

Tailleux, A., P. Duriez, J. C. Fruchart, and V. Clavey. 2002. Apolipoprotein A-II, HDL metabolism and atherosclerosis. *Atherosclerosis.* 164:1–13.

Tall, A. R., R. J. Deckelbaum, D. M. Small, and G. G. Shipley. 1977. Thermal behavior of human plasma high density lipoprotein. *Biochim. Biophys. Acta.* 487:145–153.

Thuahnai, S. T., S. Lund-Katz, D. L. Williams, and M. C. Phillips. 2001. Scavenger receptor class B, type I-mediated uptake of various lipids into cells. Influence of the nature of the donor particle interaction with the receptor. *J. Biol. Chem.* 276:43801–43808.

Wetterau, J. R., and A. Jonas. 1982. Effect of dipalmitoyl phosphatidylcholine vesicle curvature on the reaction with human apolipoprotein A-I. *J. Biol. Chem.* 257:10961–10966.

Yang, W. Y., and M. Gruebele. 2003. Folding at the speed limit. *Nature.* 423:193–197.